

# Manifold domain structure of double films with perpendicular magnetic anisotropy

D Coffey<sup>1,2,3</sup>, J L Diez-Ferrer<sup>1,2</sup>, E C Corredor<sup>1,2</sup>, J I Arnaudas<sup>1,2,3</sup>, and M Ciria<sup>2,3</sup>

<sup>1</sup>Instituto de Nanociencia de Aragón, Universidad de Zaragoza, Zaragoza, Spain.

<sup>2</sup>Departamento de Física de la Materia Condensada, Universidad de Zaragoza, Zaragoza, Spain.

<sup>3</sup>I.C.M.A, Universidad de Zaragoza and C.S.I.C., Zaragoza, Spain.

E-mail: [ciria@unizar.es](mailto:ciria@unizar.es)

## Abstract.

We present epitaxial structures made of twin nickel blocks with perpendicular magnetic anisotropy separated by a copper layer which, for some values of this interleaving layer, show domain structures with four levels of contrast in magnetic force microscopy images. This manifold domain structure implies that the magnetization in the Ni blocks, besides the parallel orientation, undergoes a non-collinear configuration with respect to each other. To explain this result we consider a magnetoelastic domain structure with  $M$  in the plane that can elude the clamping done by the substrate with an average strain of  $-42 \cdot 10^{-6}$  ( $\approx 70\%$  of the bulk value). Thus, the out-of-plane anisotropy is balanced and a biquadratic exchange coupling can stabilize non-collinear domain configurations between the Ni blocks.

PACS numbers: 75.60.Ch, 75.70.-i, 75.70.Ak, 75.70.Kw

Submitted to: *J. Phys. D: Appl. Phys.*



## 1. Introduction

The development of nanostructures including layers with perpendicular magnetic anisotropy has allowed keeping the pace of increasing the areal density in recording media [1]. These kind of layers aim to improve the performance of spintronic devices like planar nanowires [2] and nanopillar spin valves [3] since reducing the critical current for spin-transfer switching in these kind of systems appears to be more feasible than in layers with in-plane anisotropy. Patterned media for magnetic recording improves areal density by reducing the bit boundary noise of granular films, and, possibly, by means of multiple storage states [4]. Using this strategy  $2^n$  available states can be achieved, where  $n$  is the number of magnetic blocks, by using layers with different values of the effective perpendicular magnetic anisotropy constant  $K_{eff}$ .

Most of these studies have been done in structures where the magnetic layers with perpendicular anisotropy are made of Co/Pt or Co/Pd blocks, and interleaving layers suitable for large antiferromagnetic coupling, Ru [5, 6, 7, 8] or NiO [9, 10, 11]. The balance between interlayer interactions, namely magnetostatic and exchange coupling, dictates the domain configuration formed of these metastable states and tuning the oscillating exchange coupling can satisfactorily stabilize remanent states [12]. A further step is the use of blocks with competing magnetic anisotropies (easy axis perpendicular to the surface and in the film plane) to obtain artificial magnetic structures with non-collinear and not orthogonal magnetic configurations[13].

A common factor of these structures is that a tiny difference in the energy, tuned by choosing structural parameters, can be favored by a small magnetic field, resulting in a remarkable change of the magnetic configuration, therefore high order contributions to the total magnetic energy may be important to explain the magnetic state.

Here we present magnetic force microscopy images in structures in which a copper block separates two twin nickel layers with out-of-plane magnetization due to a magnetoelastic (ME) effect. We observe that the number of levels of the MFM signal changes with the thickness of the copper block, and images with two, three and up to four stable states are reported. Whereas the images with two and three levels are explained as result of dipolar and lineal exchange interaction that keep the magnetization in each Ni block perpendicular to the film plane but parallel or anti-parallel to each other, the fourfold contrast suggests the presence of domain structures with in-plane components of  $\mathbf{M}$  in the Ni blocks. The stability of these four states is explained as a result of the existence of a biquadratic exchange coupling and the formation of magnetoelastic domains that elude the clamping done by the buffer layer. Thus, the metastable deformation of the nickel lattice in each domain is able to balance the perpendicular anisotropy and the biquadratic exchange interaction stabilizes the non collinear structure.

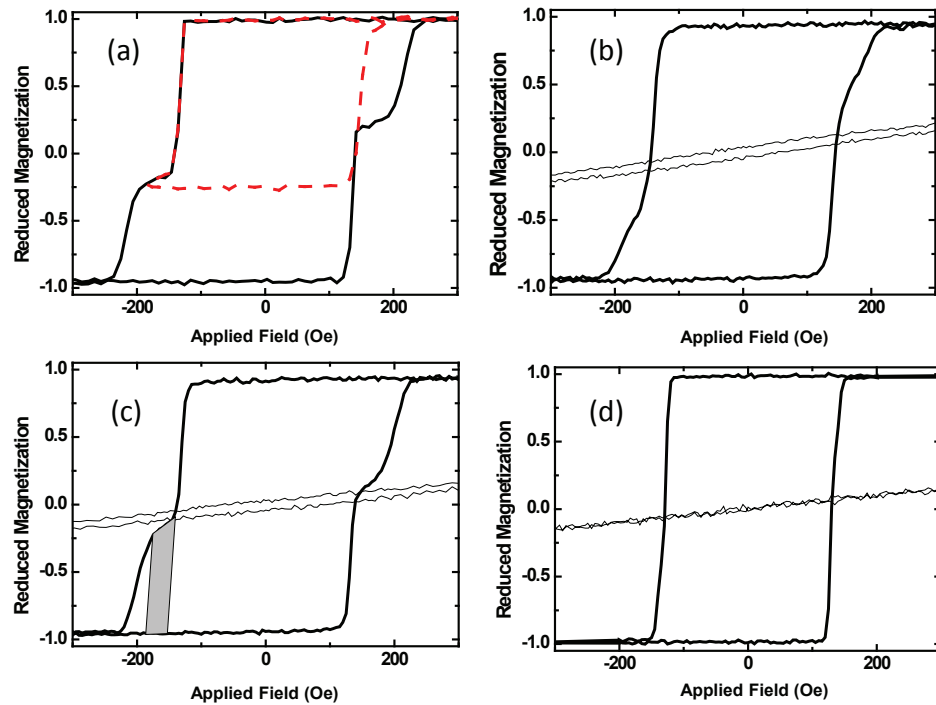


**Figure 1.** Detail of the M-H loops with H perpendicular to the plane (thick lines) for structures Ni(3 nm)/Cu( $t_{Cu}$ )/Ni(3 nm) with  $t_{Cu}$  (a) 3.5 nm, (b) 4 nm, (c) 4.5 nm and (d) 6 nm. In panel (a) a minor loop is also shown (dashed line). M-H loops with H along the film plane are also shown (thin line) for the remaining structures. The grey area in panel (c) is used to estimate the strength of the biquadratic exchange contribution (see text).

## 2. Experiment

Epitaxial Cu (5nm)/Ni (3nm)/Cu (100 nm) and Cu (5nm)/Ni (3nm)/Cu ( $t_{Cu}$ )/Ni (3nm)/Cu (100 nm) films with  $t_{Cu} = 3.5$  nm, 4 nm, 4.5 nm and 6 nm were grown on Si (001) wafers at room temperature by electron-beam evaporation in a chamber with a base pressure below  $2 \times 10^{-10}$  Torr, using a procedure reported elsewhere[14]. Hysteresis loops and domain images of the samples were taken at room temperature using a vibrating sample magnetometer (VSM) and a magnetic force microscope (MFM), respectively. Plane scans at constant average height from the sample surface are used to obtain the MFM images presented here. The short distance forces that produce the topographic profile can be minimized by adjusting the sample-tip distance, while the long distance magnetic force can still be detected in this configuration, greatly reducing the distortion of the domain structure that may happen in the more usual retrace mode.

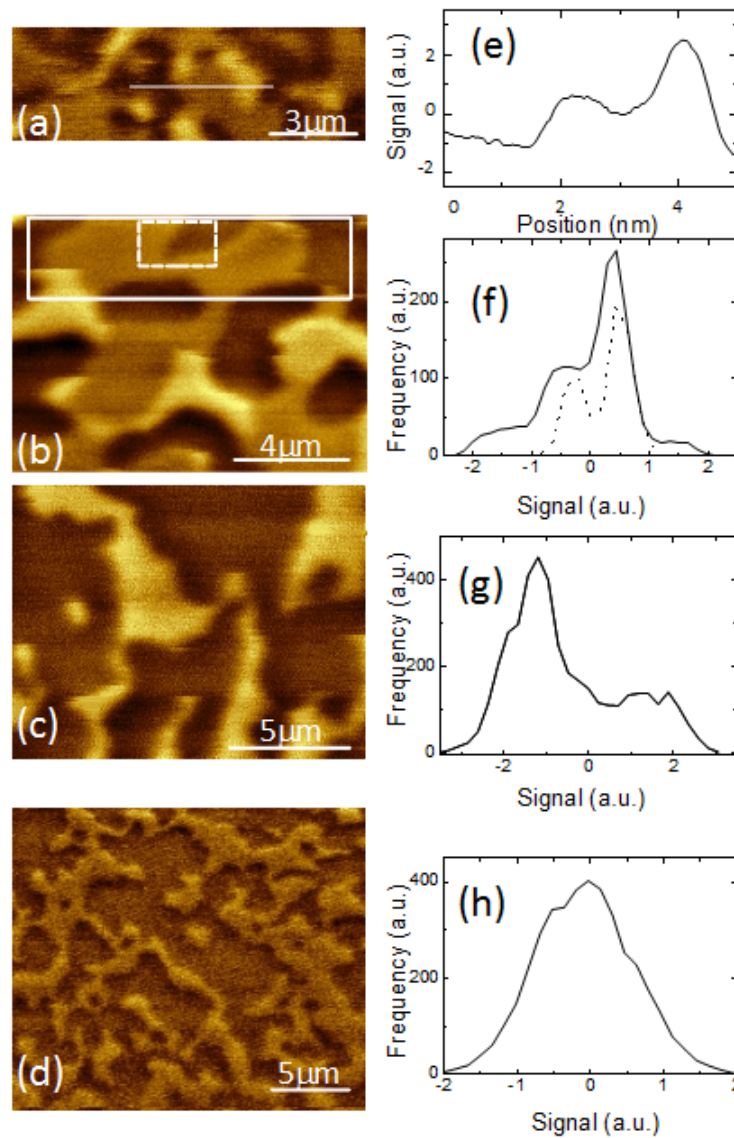
### 3. Results and Discussion

Figure 1 displays hysteresis loops for double films with the magnetic field  $H$  applied parallel (thin continuous line) and perpendicular to the film plane (thick continuous line). The remanent magnetization  $M_r$  is close to one for all the M-H loops with  $H$  perpendicular to the plane as expected for a loop taken along an easy direction; meanwhile the in-plane loops display no significant values for  $M_r$ . These findings indicate the presence of an effective magnetic anisotropy perpendicular to the film, being the value of  $K_{eff}$  about  $90 \text{ kJ/m}^3$  for all the films presented in this work [14]. The sharp change in the value of  $M$  at the value of the coercive field  $H_c$  indicates that the inversion of  $\mathbf{M}$  proceeds with the propagation of domain walls previously nucleated. For the structures with  $t_{Cu} = 3.5 \text{ nm}$  and  $4.5 \text{ nm}$  a plateau is observed during the inversion of the magnetization that, on the contrary, is absent for the structures with  $t_{Cu} = 4 \text{ nm}$  and  $6 \text{ nm}$ .

The absence of a plateau in the M-H loop for the structure with  $t_{Cu} = 4 \text{ nm}$ , between  $3.5$  and  $4.5 \text{ nm}$ , suggests that the features around  $H_c$  can be due to the presence of an oscillating interaction such as the interlayer exchange coupling (both bilinear and biquadratic). Nevertheless, the minor M-H loop, see dashed line in figure 1(a), done after saturating the sample in a positive  $H$  and applying a negative field of  $-185 \text{ Oe}$ , shows a marginal shift,  $\approx 10 \text{ Oe}$ , suggesting a small value of a bilinear exchange coupling, as could be expected for structures with interleaving copper layers larger than  $3 \text{ nm}$  [15]. The in-plane M-H loops does not show anomalies related to the plateaus observed in the hysteresis loops taken with  $H$  perpendicular to the plane [see figure 1(b)-(d)].

The MFM technique is useful in the study of the magnetism in double films with perpendicular magnetization because it has revealed parallel (P) and antiparallel (AP) orientation of  $\mathbf{M}$  between blocks [16]. Figure 2 shows images taken in the virgin state on the structures with  $t_{Cu} = 4, 4.5$  and  $6 \text{ nm}$ , and a  $3 \text{ nm}$  thick film. The structures with  $t_{Cu} = 4$  [figure 2(a)] and  $4.5 \text{ nm}$  [figure 2(b)] show three and four levels in the contrast as shown the profile [figure 2(e)] taken along the white line in figure 2(a) and the histograms shown in figure 2(f). Notice that by taking the histograms on the areas marked in figure 2(b) up to four well defined peaks can be identified in the region delimited by a straight line by only two peaks if the selected area is the dashed rectangle. For the remaining structures [figure 2(c) and (d)] two hues are observed in the images, although the observation of two well defined peaks in the histograms taken on the MFM images depend on the signal to noise ratio [figure 2(g) and (h)].

We note that these domain structures are unstable, being the stray field from the tip enough to modify the domain structures observed in figure 2. For the samples with  $t_{Cu} = 4$  and  $6 \text{ nm}$  and for the Ni thin film, the magnetic tip erases completely the domain structure in such a way that no contrast is observed after a few scans. This situation is different for the structure with  $t_{Cu} = 4.5 \text{ nm}$ . Figure 3(a) and (b) illustrate how a two states domain structure is obtained after the extreme hues areas turn into areas with the two intermediate hues due to the magnetic field from the tip.



**Figure 2.** Magnetic force microscopy images taken on Ni(3)/Cu( $t_{Cu}$ )/Ni(3) double films with  $t_{Cu}$  (a) 4 nm; (b) 4.5 nm (c) 6 nm and (d) a 3 nm thick Ni film, (e) profiles taken on image (a). (f-h) Histograms taken on the MFM images except for panel (f) where the continuous and dashed histograms correspond, respectively to the areas marked with continuous and dashed lines on image (b).

Enlarging the scan area to image untouched regions shows again the extreme contrast lost in the repeatedly scanned area, see figure 3(c). Note that while the white or black regions tend to disappear during the scanning, areas and bubbles with intermediate colors remain stable: see how the white bubble in figure 3(a) has disappeared in figure 3(b) (white ellipse) and the inverted U domain in figure 3(b) and 3(c) initially included the two extreme colors [see figure 3(a)]. Profiles taken along scan lines [see figure 3(d), continuous line] and histogram [figure 2(f), continuous line] show up to four levels or peaks if they include virgin areas and only two peaks if they are done in the scanned area [see figure 3(d), dashed line]. The domain structure achieved after the perturbation carried out by the tip has a signal that is in between the extremal values observed in the virgin state. The signal has maxima and minima at about 1.5 and -1.5 and the intermediate signal values are around 0.6 and -0.6 [see arrows in figure 3(d)]. The persistence of metastable states seems to be associated with the hysteresis loop [see figure 1], since similar images, showing four states, have been taken for the  $t_{Cu} = 3.5$  nm structure.

Domain configurations have been explained by means of a magnetic state where the magnetization vector of the top and bottom Ni blocks, namely  $\mathbf{m}_{top}$  and  $\mathbf{m}_{bot}$ , are considered homogeneous along the normal direction because the nickel thickness is smaller than the nickel exchange length ( $\sqrt{A/K} \approx 10$  nm, with  $A = 10^{-11}$  J/m and  $K = 90$  kJ/m<sup>3</sup>). For MFM images with three hues  $\mathbf{m}_{top}$  and  $\mathbf{m}_{bot}$  are always perpendicular to the plane but may be parallel or antiparallel to each other. For the latter configuration the up-down or down-up domains provides the same contrast in the MFM image, because the dipolar field coming from the two AP configurations is much smaller (1/100 for scan distances in the range of 50-100 nm) than that coming from double films with P orientation [16] or from structures with an odd number of AP blocks [7].

For structures with  $t_{Cu} = 3.5$  and 4.5 nm, assigning to  $\mathbf{m}_{top}$  and  $\mathbf{m}_{bot}$  an orientation perpendicular to the plane and parallel to each other will produce domains with extreme signal ( $\pm 1.5$ ), while a non collinear distribution with a net perpendicular component could explain the intermediate signals ( $\pm 0.6$ ), see sketches in figure 4(a). Nevertheless, the actual orientation of  $\mathbf{m}_{top}$  and  $\mathbf{m}_{bot}$  can not be established, due to the dependence of the magnetic signal with the lateral dimension of the domain structure [17], smaller domains giving rise to a larger signal; and due to the screening of the perpendicular field of the bottom block by a non perpendicular upper magnetic block.

The AP configuration is the result of a competition between antiferromagnetic exchange coupling and the dipolar interaction [6, 10, 18] or the result of two uncoupled films with different coercive field. We discard the latter consideration because the structure with the larger value of  $t_{Cu}$  inverts  $\mathbf{M}$  almost completely at the coercive field value. Therefore, the observation of images with larger number of levels in double films suggests the presence of structures where  $\mathbf{m}_{top}$  and  $\mathbf{m}_{bot}$  no longer are perpendicular to the plane and therefore additional magnetic contributions in the energy balance.



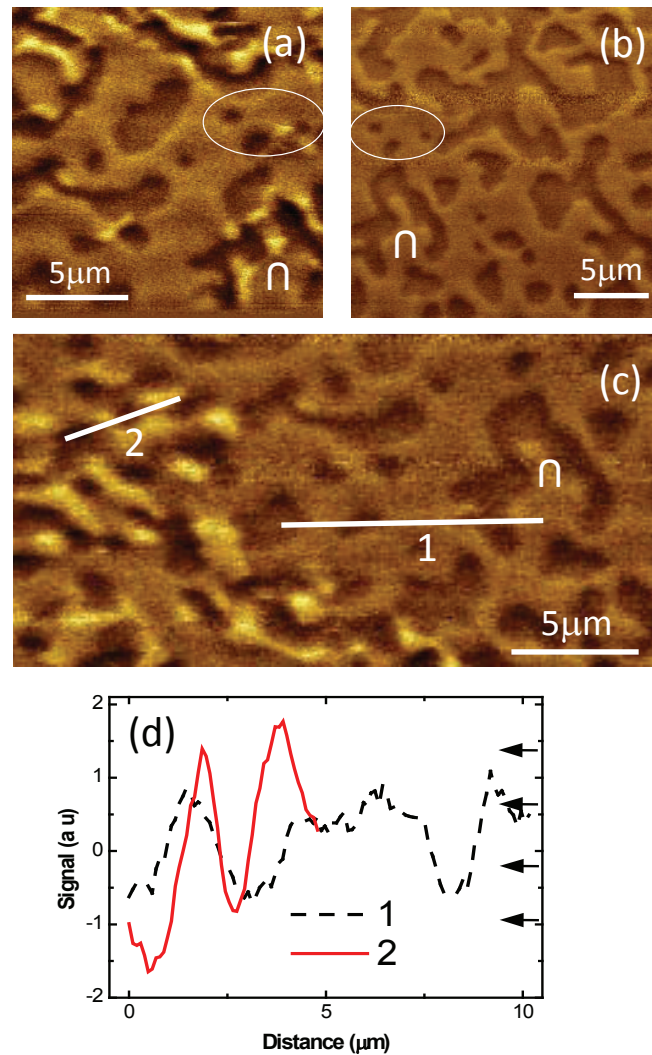


**Figure 3.** (a)-(c)MFM images taken on Ni(3)/Cu(4.5)/Ni(3) double film on similar areas. (d) Profiles taken on image (c)

#### 4. Model

In order to explain the manifold contrast observed in the MFM images we consider the relevant contributions to the energy density  $e_{mag}$  that determine the orientation of  $\mathbf{M}$  in the Ni blocks. It is well established that including in  $e_{mag}$  the magnetostatic energy  $e_{ms}$  term, an out-of-plane magnetic anisotropy  $K \sin^2 \theta$  ( $\theta$  is the angle between  $\mathbf{M}$  and the film normal) and the domain wall energy, the lowest energy domain structure consists in regions with AP magnetization pointing perpendicularly to the plane, as is observed in Cu/Ni/Cu thin films [19]. Including an interleaving block between the magnetic blocks has required the presence of a bilinear exchange term in the magnetic energy,  $-J_1 \mathbf{m}_{top} \mathbf{m}_{bot}$ , ( $J_1$  is the bilinear exchange constant) to explain the contrast in MFM images taken in Co/(Pt,Pd)/Ru based multilayers. In these films with AP orientation

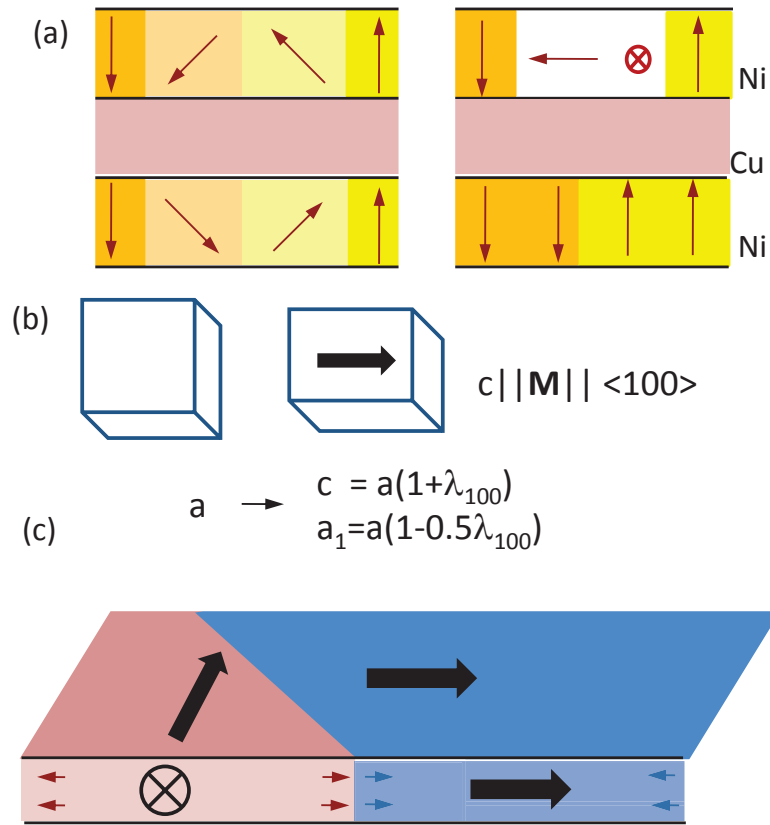


**Figure 4.** (a) Sketch of domain configurations that can provide 4 levels in the MFM signal. The parallel domains provide the extremal values while the domains forming 90 degrees provide two intermediate levels. The configuration on the left panel minimizes the dipolar coupling between the nickel blocks. (b) Sketch of the tetragonal distortion of a cubic material and the resulting lattices parameters. The values of  $c$  and  $a_1$  are particularized for an irreducible tetragonal magnetostrictive deformation with value  $\lambda_{100}$ . (c) Stress distribution for a film with a  $90^\circ$  domain wall, the thick arrows stand for the magnetization or electric polarization vector. The small arrows indicate the in-plane stress component at a section of the film within each domain for a material with negative magnetostriction.

of  $\mathbf{m}_{top}$  and  $\mathbf{m}_{bot}$ , the observed contrast has been attributed to the domain wall shape [7]. A biquadratic term,  $-J_2(\mathbf{m}_{top}\mathbf{m}_{bot})^2$ , where  $J_2$  is the biquadratic exchange coupling constant [20] favors a  $90^\circ$  angle  $\phi$  between  $\mathbf{m}_{top}$  and  $\mathbf{m}_{bot}$ . Thus competing interactions require, to find the equilibrium configuration, minimizing the total energy per block:

$$e_{mag}/t_{Ni} = e_{ms}/t_{Ni} + K \sin^2 \theta / t_{Ni} - J_1 \mathbf{m}_{top} \mathbf{m}_{bot} - J_2 (\mathbf{m}_{top} \mathbf{m}_{bot})^2 \quad (1)$$

An estimation of the value of  $J_2$  required to obtain angles of  $\phi=90^\circ$  can be obtained assuming first that the biquadratic exchange contribution is able to balance the magnetic



anisotropy, secondly that  $e_{ms}$  is the value for a single domain ( $\approx (1/2)\mu_0 M^2 \cos^2\theta$ ), and finally that  $J_1$  is small. This gives  $J_2 \approx -0.14$  mJ/m<sup>2</sup>, a very large value considering the range of thicknesses of copper for which the presence of noncollinear structure is proposed,  $t_{Cu} \approx 3.5 - 4.5$  nm, and that typical values for  $|J_2|$  ranges between 0.01 - 0.1 mJ/m<sup>2</sup>, being the larger values found at thicknesses of the interlayer block no larger than 1 nm [21].

Noting that the image with up to four different levels of the MFM signal is observed as a metastable state since it is modified by the application of magnetic field, we consider the modification of the energy  $e_{mag}$  arisen from a configuration of magnetic domains. Since the elastic and magnetoelastic energies are the most relevant contributions to understand the magnetic configuration in the Ni layers, we analyze the variation of these contributions if  $\mathbf{M}$  would lie in the basal plane inducing a tetragonal magnetostrictive distortion in the magnetic domains, see figure 4(b), with the domains forming 90° domain walls, figure 4(c). This mechanism is similar to the twin related domain formation that releases the elastic energy in tetragonally strained ferroelectric and ferroelastic epitaxial films [22], by the formation of structures of domains with the  $\mathbf{c}$  axis of the tetragonal domain related to neighbor domains by a rotation of 90 degrees. This mechanism has been suggested to explain the domain configuration in magnetostrictive Co<sub>50</sub>Fe<sub>50</sub>/Co<sub>80</sub>B<sub>20</sub> films [23] and the magnetic order in Dy films (a crystal with hcp structure) grown on top of non-magnetic Y-Lu films [24]. These magnetoelastic domain structures gives rise to a in-plane strain distribution that was observed in Dy/Lu superlattices by the measuring of a three-fold splitting in the diffraction peaks due to domains with  $\mathbf{M}$  pointing along the six in-plane easy directions [25].

In all the cases the domain patterning consists in volumes with alternating orientation of the magnetization or the polarization vector that due to the stress state associated with the  $\mathbf{M}$  or  $\mathbf{P}$  alternate compression and tension states inside each domain [see figure 4(c)]. Because the boundary for the in-plane lattice parameter imposed by the seed layer has to be fulfilled it has been suggested that the relaxation on the strained film can take place first at the domain boundaries that act as displacement dampers [22] and through the generation of anisotropic networks of linear densities of misfit dislocation [26].

The epitaxial strain in the film due to the energy balance between elastic and plastic contributions to the total energy is taken as reference. The thickness of the Cu seed layer,  $t_{seed}$ , much larger than that value for Ni blocks, indicates that homogeneous stresses in the nickel layer have a negligible effect on the system because their weight on the total energy goes with a factor  $t_{Ni}/(t_{Ni}+t_{seed})$ . Thus, we evaluate the variation of the elastic density energy if the magnetostrictive strain is allowed to exist in the Ni film by the formation of a set of  $i$  domains, each one with a volume  $v_i$  and with  $\mathbf{M}$  in the plane along  $\langle 100 \rangle$  directions, see figure 4(c). Inside each domain, to the epitaxial strain components  $\varepsilon_{jk}^0$  (with  $j, k = x, y, z$  defined along the  $\langle 100 \rangle$  directions) the magnetostrictive deformations  $\varepsilon_{jk}^{me}$  are added, getting for the strain components  $\varepsilon_{jk} = \varepsilon_{jk}^0 + \varepsilon_{jk}^{me}$ . Taking the expression of the elastic energy for a crystal with cubic symmetry, inserting the strain components  $\varepsilon_{jk}$ , keeping only contributions linear in the magnetostrictive strain,

and considering that the nickel blocks are under a biaxial strain with the stress  $\sigma_{zz}=0$ , we have that  $\varepsilon_{xx}^0 = \varepsilon_{yy}^0 = \varepsilon^0$ ;  $\varepsilon_{zz}^0 = -(2c_{12}/c_{11})\varepsilon^0$ ;  $\varepsilon_{xy}^0 = \varepsilon_{yz}^0 = \varepsilon_{zx}^0 = 0$ , where  $c_{11}$  and  $c_{12}$  are elastic constants, the next equation is obtained for the energy released in each domain:

$$\Delta e_i = (\varepsilon_{xx}^{me} + \varepsilon_{yy}^{me})\varepsilon^0 \left[ (c_{11} + c_{12}) - 2\frac{c_{12}^2}{c_{11}} \right] \quad (2)$$

Note that the more usual magneto-elastic corrections effects, that go with  $(\varepsilon_{jj}^{me})^2$ , result negligible compared with the terms of Equation (2) due to the strong internal deformation,  $\varepsilon^0$  that for our films is  $\varepsilon^0 \approx 2.1 \cdot 10^{-2}$  [14], while  $\varepsilon_{ii}^{me} \sim 6 \cdot 10^{-5}$  [27].

The relationship between magnetostrictive strain  $\varepsilon^{me}$ , irreducible deformations of the cubic lattice, orientation of  $\mathbf{M}$  and the measurement direction is,

$$\varepsilon^{me}(\alpha, \beta) = (3/2)\lambda_{100}[\alpha_x^2\beta_x^2 + \alpha_y^2\beta_y^2 + \alpha_z^2\beta_z^2 - (1/3)] + 3\lambda_{111}(\alpha_x\alpha_y\beta_x\beta_y + \alpha_y\alpha_z\beta_y\beta_z + \alpha_z\alpha_x\beta_z\beta_x) \quad (3)$$

where the  $\alpha'_i$  correspond to the cosines of  $\mathbf{M}$ , the  $\beta'_i$  to the cosines of the measurement direction and  $\lambda_{100}$  and  $\lambda_{111}$  are the magnetostriction cubic coefficients that stand, respectively, for the tetragonal and rhombohedral distortions of the cubic lattice. If  $\mathbf{M}$  is along the  $\langle 10 \rangle$  in-plane direction, we obtain, respectively, for the strain components parallel and transversal to  $\mathbf{M}$   $\varepsilon_{10}^{me} = \lambda_{100}$  and  $\varepsilon_{01}^{me} = -\lambda_{100}/2$ , getting for  $\Delta e_i = (1/2)\varepsilon^0 C \lambda_{100,i}$ , where  $C$  includes the elastic constants combination in the bracket of Equation (2). The total variation of the density energy is evaluated as a sum over the  $i$  domains with fraction volume  $v_i$  in which the film is divided:  $\Delta e = \sum_i v_i \Delta e_i$ . Defining the average value of  $\lambda_{100}$  as  $\langle \lambda_{100} \rangle = \sum_i (1/2)\lambda_{100,i}v_i$ , the expression  $\Delta e = (1/2)\varepsilon^0 C \langle \lambda_{100} \rangle$  is obtained.

For the Ni/Cu system  $\Delta e$  release energy ( $\Delta e < 0$ ), since  $\varepsilon^0 \approx 0.021$  [14], and  $\lambda_{100}$  is negative [27]. If  $\Delta e$  were able to keep one of the magnetic layers with the domains in the film plane, it should overcome  $K_{eff} \approx 90 \cdot 10^3 \text{ J/m}^3$ . The value of  $\langle \lambda_{100} \rangle$  in the film in order to release enough elastic energy to match  $K_{eff}$  is  $\approx -42 \cdot 10^{-6}$  (with  $c_{11} = 2.5 \cdot 10^{11} \text{ J/m}^3$  and  $c_{12} = 1.6 \cdot 10^{11} \text{ J/m}^3$  [28]), a value clearly smaller than the bulk  $\lambda_{100}$  ( $-60 \cdot 10^{-6}$  [27]) and three orders of magnitude smaller than  $\epsilon_0$ . This calculation indicates that this configuration would balance the out-of-plane magnetic anisotropy because it is compatible with the reported values for  $\lambda_{100}$ . Thus, beside domain configuration with  $\mathbf{m}_{top}$  and  $\mathbf{m}_{bot}$  perpendicular to the plane, either parallel or antiparallel to each other that can explain the MFM images for the structures with  $t_{Cu} = 6$  and  $4\text{nm}$ , respectively, more sophisticated structures of domains with canted orientation of the magnetization with in-plane and out of plane components of  $\mathbf{M}$  would be also possible if the coupling between the Ni blocks favors a non co-linear orientation of  $\mathbf{m}_{top}$  and  $\mathbf{m}_{bot}$ .

We stress that when  $\mathbf{M}$  is uniform the copper lattice clamps the nickel lattice to a certain value due to the energy balance between elastic and plastic contributions to the film total energy. Only during a process of inversion of the  $\mathbf{M}$  the proposed domain configuration could take place. Thus, in a scenario where the perpendicular anisotropy is compensated by the formation of magnetoelastic domains, second order interactions

favoring non-collinear states are required to stabilize the multilevel domain patterns proposed in figure 4(a). The biquadratic exchange interaction that favors a orientation of 90 degrees between  $\mathbf{m}_{top}$  and  $\mathbf{m}_{bot}$ , even being small in absolute value, could play the capital role of stabilizing non-collinear structures and be responsible for the plateaux observed in the MH loops since additional Zeman energy, supplied by increasing the magnetic field, is needed to unlock the non-collinear state. In order to estimate the strength of  $J_2$  we consider that the energy associated to the area  $A$  in the M-H loops due to the presence of plateaux [see figure 1(c)] can be assigned to the biquadratic term, and  $A = -J_2(\mathbf{m}_{top}\mathbf{m}_{bot})^2/t_{Ni}$ , getting  $J_2 \approx -0.005$  mJ/m<sup>2</sup>, a reasonable value for this kind of interaction.

## 5. Summary

Magnetic structures with four well defined values have been observed by magnetic force microscopy in twin nickel blocks with an interleaving copper layer. This structure is explained as the result of a domain configuration that includes magnetoelastic domains with in-plane components and biquadratic exchange coupling. We note that engineering layers with metastable domain configurations based on the strain state of the magnetic film makes this kind of materials suitable to be used in conjunction with piezoelectric materials that modify their dimensions by means of an electric field and, therefore, the strain state and the ME anisotropy energy in the magnetic film.

## Acknowledgments

This work has been supported by Spanish MICINN (Grants No. MAT2006-07094 and MAT2009-10040) and DGA (Grants E81 and PI049/08) and Fondo Social Europeo.

## References

- [1] Piramanayagama S N 2007 *J. Appl. Phys.* **102**, 011301.
- [2] Ravelosona D, Lacour D, Katine J A, Terris D B, and Chappert C 2005 *Phys. Rev. Lett.* **95**, 117203.
- [3] Mangin S, Henry Y, Ravelosona D, Katine J A, and Fullerton E E 2009 *Appl. Phys. Lett.* **94**, 012502.
- [4] Albrecht M, Hu G, Moser A, Hellwig O, and Terris B D 2005 *J. Appl. Phys.* **97**, 103910.
- [5] Hellwig O, Kirk T L, Kortright J B, Berger A and Fullerton E E 2003 *Nature Mater.* **2**, 112.
- [6] Hellwig O, Berger A, and Fullerton E E 2003 *Phys. Rev. Lett.* **91**, 197203.
- [7] Hellwig O, Berger A, Kortright J B and Fullerton E E 2007 *J. Magn. Magn. Mater.* **319**, 13.
- [8] Fu Y, Pei W, Yuan J, Wang T, Hasegawa T, Washiya T, Saito H and Ishio S 2007 *Appl. Phys. Lett.* **91**, 152505.
- [9] Liu Z Y and Adenwalla S 2003 *Phys. Phys. Lett.* **91**, 037207.
- [10] Baruth A, Yuan L, Burton J D, Janicka K, Tsymbal E Y, Liou S H and Adenwalla S 2006 *Appl. Phys. Lett.* **89**, 202505.
- [11] Liu Z Y, Li N, Zhang F, Xu B, He J L, Yu D L, Tian Y J, and Yu G H 2008 *Appl. Phys. Lett.* **93**, 032502.

- [12] Baltz V, Rodmacq B, Bollero A, Ferré J, Landis S and Dieny B 2009 *Appl. Phys. Lett.* **94**, 052503.
- [13] Yildiz F, Przybylski M and Kirschner J 2009 *Phys. Rev. Lett.* **103**, 147203.
- [14] Corredor E C, Diez-Ferrer J L, Coffey D, Arnaudus J I and Ciria M 2010 *J. Phys. Conf. Ser.* **200**, 072019.
- [15] Bloemen P J H, van Dalen F L, de Jonge W J M, Johnson M T and van de Stegge J 1993 *J. Appl. Phys.* **73**, 5972.
- [16] Hamada S, Himi K, Okuno T and Takanashi K 2002 *J. Magn. Magn. Mat.* **240**, 539.
- [17] Hug H J, Stiefel B, van Schendel P J A, Moser A, Hofer R, Martin S, Güntherodt H J, Porthun S, Abelmann L, and Lodder J C, Bochi G and O'Handley R C 1998 *J. Appl. Phys.* **83**, 5609.
- [18] Janicka K, Burton J D and Tsymbal E Y 2007 *J. Appl. Phys.* **101**, 113921.
- [19] Bochi G, Hug H J, Paul D I, Stiefel B, Moser A, Parashikov I, Güntherodt H J and O'Handley R C 1995 *Phys. Rev. Lett.* **75**, 1839.
- [20] Demokritov S O 1998 *J. Phys. D: Appl. Phys.* **31** 925.
- [21] Fuss A, Demokritov S O, Grünberg P and Zinn W 1992 *J. Magn. Magn. Mater.* **103** L221.
- [22] Pompe W, Gong X, Suo Z and Speck J S 1993 *J. Appl. Phys.* **74**, 6012.
- [23] McCord J, Schäfer R, Frommberger M, Glasmachers S and Quandt E 2004 *J. Appl. Phys.* **95**, 6861.
- [24] Tsui F and Flynn C P 1993 *Phys. Rev. Lett.* **71**, 1462.
- [25] Beach R S, Borchers J A, Matheny A, Erwin R W, Salamon M B, Everitt B, Pettit K, Rhyne J J and Flynn C P 1993 *Phys. Rev. Lett.* **70**, 3502.
- [26] Speck J S and Pompe W 1994 *J. Appl. Phys.* **76**, 466.
- [27] Lee E W and Asgar M A 1971 *Proc. R. Soc. Lond. A.* **326**, 73.
- [28] Bozorth R M, Mason W P, McSkimin H J and Walker J G 1949 *Phys. Rev.* **75**, 1954.